OPEN ACCESS
ACTA METALLURGICA SLOVACA
2025, VOL. 31, NO. 4, 225-233
SCICELL

RESEARCH PAPER

Evaluation of the effect of TIG surface quenching process of S45C steel on the hardness of cylindrical surface layers by Taguchi method

Van-Thuc Nguyen[1], Pham Son Minh[1], Huynh Do Song Toan[1], Nguyen Ho[2,]*

[1] HCMC University of Technology and Education, Ho Chi Minh City 71307, Viet Nam;
[2] PhD. Student, Faculty of Mechanical Engineering, HCMC University of Technology and Education, Ho Chi Minh City 71307, Viet Nam

*Corresponding author: hon.ncs@hcmute.edu.vn, tel.: +84977951638, Faculty of Mechanical Engineering, HCMC University of Technology and Education, 71307, Ho Chi Minh City, Viet Nam

Received: 09.09.2025
Accepted: 22.10.2025

ABSTRACT

This study investigates the influence of current intensity, relative travel speed of the TIG torch on the cylindrical S45C steel surface, and axial travel speed on hardness distribution in deep layers after arc quenching. The process forms three distinct zones: quenched, heat-affected, and base metal. The quenched zone transforms from the original ferrite–pearlite structure into martensite, residual austenite, and bainite. The heat-affected zone contains bainite, pearlite, and ferrite. These phase variations result from rapid heating and cooling. Hardness evaluation across 25 cases shows the 0.4–0.6 mm range provides the most stable and highest hardness. Taguchi analysis reveals that axial travel speed primarily affects arc width and has little effect on hardness depth. In contrast, current intensity strongly affects heat input: higher current increases heat input from the TIG tip, while higher relative travel speed reduces it. The highest hardness values were observed at different depths: 37.7 HRC at 0.2 mm (case 17), 38.3 HRC at 0.4 mm (case 21), and 42.6 HRC at 0.6 mm (case 2). At deeper layers, hardness increased significantly, with 43.6 HRC at 0.8 mm (case 1) and 41.9 HRC at 1 mm (case 1). The results of the study confirm that variations in current intensity and relative travel speed play decisive roles in determining the hardness distribution of S45C steel subjected to TIG arc quenching.

Keywords: surface hardness, current intensity, Cylindrical, heat treatment.

INTRODUCTION

Surface quenching of medium-carbon steel is a widely used industrial technique [1]. The steel surface will be heated to a specific temperature to transform into austenite, then rapidly cooled to form hard phases [2]. After steel surface quenching, the surface mechanical properties change from their original state due to a phase change, resulting in higher hardness and increased surface abrasion resistance. At the same time, the core retains its original mechanical properties [3]. There are many surface-quenching methods, including flame, induction, laser, electron beam, and plasma [4-8].

In recent years, a new surface-quenching method has emerged that uses an electric arc energy source [9]. This method is similar to the laser and electron beam methods in that it uses a large amount of heat generated by an electric arc to heat the surface material rapidly, then rapidly cool it using the part itself [10-11]. Therefore, the surface quality will be similar to that of laser, but the investment and operating costs will be much lower [12].

Safonov and Mironova [13] used arc energy to cool the surface of low-carbon steel. The steel grades used were 09G2, 20L, and 20FL with a carbon content of about 0.2%. The study was carried out by changing two parameters: travel speed from 80-180 m/h and current intensity from 180-330 A. The process overlapped the quenching zone by about 30% -50%. After surface quenching by electric arc, the hardness in the hard zone ranged from 3900 to 8800 MPa, depending on the process parameters. The depth of the hard zone ranged from 0.7 to 1mm, corresponding to the microstructure of the hard zone being martensite-residual austenite. The martensite phase has an interstitial needle-shaped structure and is the residual austenite phase. The residual austenite phase accounts for 15-20% by volume when analyzed by X-ray.

The surface hardness after quenching depends on the input heat. The input heat depends on factors such as the heat generated by the electric arc tip and the travel speed. In which the heat generated from the TIG tip depends mainly on the current intensity [14]. According to Nguyen's moving heat source model [15], travel speed is an important factor affecting input heat, as travel speed increases, input heat decreases.

Kumar et al. [16] modified the surface of AISI 4340 steel by generating heat from an electric arc during TIG welding. The study was carried out at different current levels (80, 100, 120, 140 A) and travel speeds (6, 9, 12, 15 cm/min). These parameters will give different heat input levels. The results showed that the surface hardness increased significantly, reaching 720 HV for single quenching and 445 HV for multiple quenching compared to the initial hardness of 250 HV. In addition, the depth of the hardened zone increased significantly to 1.5-3.5 mm. The study also showed that the greater the heat input, the deeper the modified layer, but the surface hardness decreased due to the reduced cooling rate.

Mikheev et al. [17] studied the surface hardening of steels 20, 40, 65G, and U8 using an electric arc power source. The input parameters studied were 100-250 A for the current intensity and 0.01-5 m/s for the travel speed between the TIG tip and the workpiece. The results showed that the maximum achievable hardness was 10 GPa compared to the initial hardness of 2 GPa. The optimal travel speed range to achieve the highest hardness was 0.6-0.9 m/s. However, at this travel speed range, the depth of the hardened layer was only 0.3-0.4 mm. To achieve a depth greater than 0.5 mm, the travel speed must be below 0.03 m/s. In addition, the study confirmed that the hardened surface exhibited 4 times the wear resistance of the untreated surface. This benefit is due to the increase in surface hardness by the electric arc, which results in a higher wear resistance of the part.

At the same time, Kumar et al. [18] examined the tensile and fatigue properties of AISI 4340 steel after TIG surface quenching. The results confirmed that increasing the heat input decreased the yield strength but increased the ductility and impact toughness of the steel after quenching. The control of heat input via two parameters—current intensity and travel speed — facilitated the formation of the desired microstructure, a combination of martensite and bainite matrix. These are the two phases that enhance the wear resistance, fatigue strength, and corrosion resistance of the steel surface after the arc-quenching process. [19].

From the above studies, controlling two key parameters in the surface quenching process — current intensity and moving speed — is extremely important, as they directly affect the input heat. These two parameters directly affect the hardness and the depth of the hardened layer. Optimizing these two parameters is extremely important in the surface

quenching technique using an electric arc. Meanwhile, the optimization tool for testing the surface hardness using the Taguchi method is very reliable [20]. In particular, the surface after being quenched by an electric arc cannot be used immediately because the heat from the arc tip causes melting [16, 18-19]. Therefore, it is necessary to remove the initial layers, and it can only be used in the lower layers. Therefore, evaluating the influence of input parameters in lower layers is extremely important but has not been previously studied.

In addition, the cylindrical surface is widely used in industry. The quenching of the tubular surface to increase its hardness has many characteristics that differ from those of the flat surface [21]. Dong Ju Kim et al. [22] conducted a study of heat transfer on three surface types: convex, concave, and flat. The results showed that the curved surface had a better heat transfer rate from the scanning beam than the flat surface. This process greatly supports the rapid cooling rate of the curved surface. Meyghani and Awang [23] studied the thermal behaviour during friction stir welding of two flat and curved surfaces of AA6061-T6 alloy. The conclusion drawn from this study shows that the curved surface always has a temperature 50-80 ^{0}C lower than the flat surface. This directly affects the quenching process of the tubular surface compared to the flat surface due to this temperature difference. Therefore, the study of the quenching of the tube surface by an electric arc is highly meaningful for expanding industrial applications.

The recent discovery of Thuc et al. [24] also shows that the width of the surface quenched by arc ranges from 2.3 mm to 6.5 mm, depending on process parameters such as current intensity, arc length, travel speed, pulse time, and gas flow rate. Therefore, when using the surface of a cylindrical part with a relative length, achieving an even-quenched surface and an optimal time to quench the entire surface are difficult. One solution that has been applied is cylindrical steel quenched by a combination of two methods, rotational and axial translation, to optimize the surface quenching time to avoid interruptions by the group of authors Leonardo et al. [25]. This research used a laser (a method like arc) to harden the surface, using a new laser based on the ring-point geometry, on AISI 1040 bars with diameters of 20 mm and 30 mm. The martensite layers are very hard, deep, and uniform in the axial direction. This can completely replace the induction quenching method and provide a new direction for arc quenching.

With the advantages and disadvantages mentioned above, this study will overcome the disadvantages of small, uneven cooling zones by using axial and rotary travel speeds. The hardness is evaluated layer by depth by cutting layers with different surface depths. In addition, the Taguchi evaluation method is also used to assess the influence of process parameters affecting the heat generation process and the heat input, such as current intensity, axial motion speed, and rotation speed of the cylindrical steel, for more effective evaluation. Evaluation of microstructural materials after surface quenching is also studied in depth. The research results will provide more insight into this method and move closer to industrial application, helping engineering technology engineers understand and apply it.

EXPERIMENTAL METHODS

Medium-carbon steel cylindrical S45C is used for the arc-quenching process, with a diameter of 76 mm, a thickness of 4.8 mm, and a length of 500 mm. **Table 1** shows the nominal chemical composition of a S45C steel cylinder. The samples are installed on a 3-jaw chuck and a center support at one end. The arc is generated by the TIG head of the welding machine, and a CNC machine controls both the test piece and the TIG head. This study will perform the surface quenching of S45C steel cylindrical by electric arc and optimize the processing parameters of electric intensity (A), the axis travel speed (V1) and rotation travel speed (V2) of S45C steel cylindrical (**Fig. 1a**). The test voltage was fixed at 80 V, the arc length was fixed at 1.5 mm, the shielding gas flow rate was 12 l/min, and the cooling water temperature was about 30 ^{0}C. After the surface quenching process by electric arc (**Fig. 1b**), the surface of the S45C steel cylinder will be machined 5 times, each time the cutting depth is 0.2 mm (**Fig. 1c**). The turning process was carried out at a speed of 80 rpm and uses a cooling water solution to avoid the impact of cutting heat on the testing process. After each 0.2 mm depth cut, the part will be measured for surface hardness at 10 points on the axial hardening zone, each point 3 mm apart. Rockwell hardness testing was performed using a Rockwell hardness tester HR-150A, Yisite, Shenzhen, China. The surface hardness of the initial sample was 90 HRB, equivalent to about 193 HV. Before performing the depth-hardness evaluation of the samples, preliminary evaluations were conducted to assess the hardened zone depth and its microstructure. The parameters for the above studies included a current intensity of 130 A, an axial travel speed of 2 mm/min, and a rotational travel speed of 460 mm/min. Microstructural analysis was performed using an Oxion OX.2153-PLM microscope (EUROMEX, Netherlands). In addition, the Oxion OX.2153-PLM microscope was also used for depth testing when combined with IMAGE software. A JEOL 5410 LV (Japan) scanning electron microscope (SEM) was used to observe the sample surface.

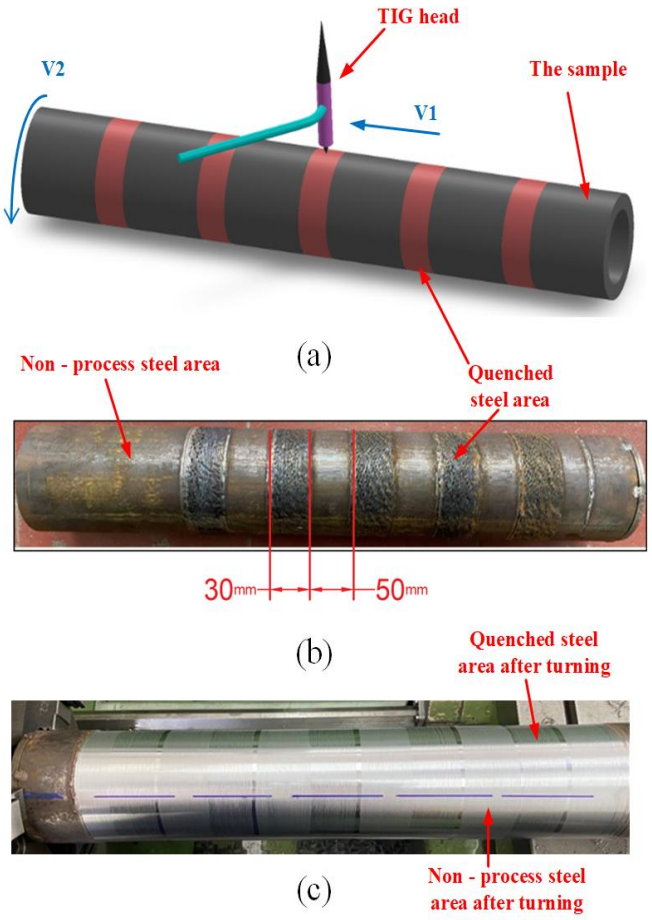

Fig. 1 Equipment and process of surface quenching test for S45C steel cylindrical: (a) Surface quenching process, (b) Surface of S45C steel cylindrical after arc quenching and (c) Steel cylindrical after turning the surface layer with a depth of 0.2 mm

Table 1 Chemical composition of S45C steel samples.

Weight %	C	Si	Mn	P	S	Ni	Cr
S45C	0.42-0.50	0.17-0.37	0.5-0.8	0.035 max	0.035 max	0.25 max	0.25 max

RESULTS AND DISCUSSION

Microstructure of the hardened sample

Fig. 2 shows the test results of the depth and microstructure of the test sample. **Fig. 2a** shows the test specimen after cutting, and the surface quenching depth of the S45C steel pipe was measured by arc. There were 10 points for depth measurement. **Table 2** shows the results of the surface depth measurement of the S45C steel tube of the test sample. The depth of the modified zone ranges from 1127 µm to 1642 µm, with an average of 1437 µm.

Table 2 Depth values of the hardened layer after surface quenching test

Measuring position	Depth of hardened zone (µm)
1	1642
2	1642
3	1611
4	1409
5	1394
6	1329
7	1269
8	1127
9	1324
10	1626
Average Hard Zone Depth: 1437 µm	

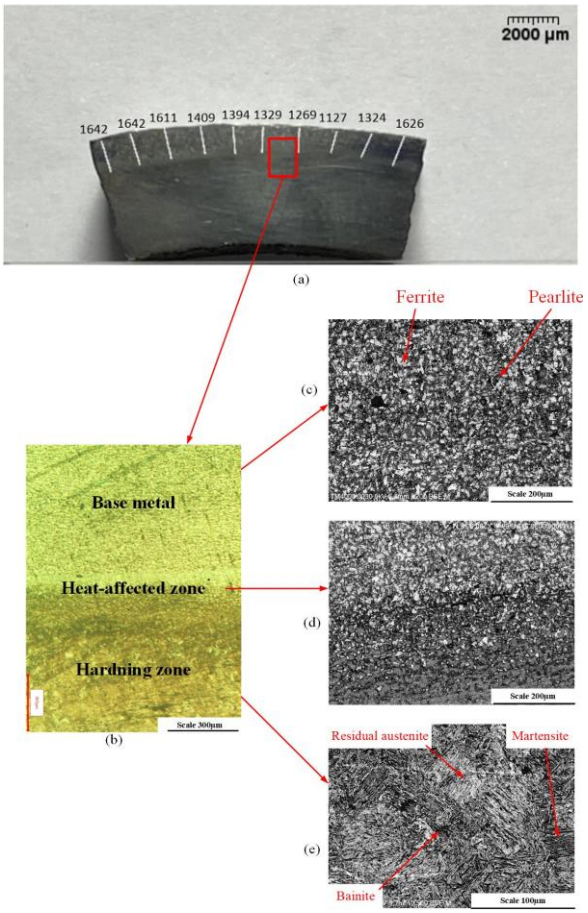

Fig. 2 The test results of the depth and microstructure of the test sample. (a) The depth of the hardened zone of the surface quenching process, (b) Microstructure of the hard zone as examined by microscope, (c) Microstructure of the base metal zone, (d) Microstructure of the heat-affected zone, (e) Microstructure of the hardening zone.

There were 3 zones with different microstructures: the hardening zone, the heat-affected zone, and the base metal zone, as shown in **Fig. 2b** under a microscope. The base metal has a 2-phase structure, which is pearlite with a dark color and ferrite with a light color, which is the original microstructure of the medium-carbon steel [26] as shown in **Fig. 2c**. **Fig. 2d** is the microstructure of the heat-affected zone, which is the transformation zone from the base metal to the hardened area. This zone consists of a bainite phase with a brown color and a ferrite phase with a brighter color, which is consistent with Kumar et al. [16] report. The hardening zone has a structure consisting of 3 phases [18-19], which are martensite phase, bainite phase, and residual austenite phase as shown in Figure 2e. The martensite phase has a needle-shaped structure [13, 17], and the la phase mainly makes the hard surface [2]. The residual austenite phase has a brighter color, and the bainite phase has a dark color. The appearance of multiple phases and multiple regions after quenching is due to the heat input and cooling rate.

Hardness measurement results by depth

Table 3 is the result of measuring the hardness according to the depth of 5 turnings, corresponding to 1 mm depth compared to the surface of the S45C steel tube. **Fig. 3** shows the hardness profile as a function of depth, derived from the results in **Table 3**.

Fig. 3a is the result of measuring the hardness of 25 samples when using different arc quenching process parameters. This figure shows that the lowest hardness is 29.3 HRC, corresponding to case 3; and the highest reaches 37.7 HRC, corresponding to case 17. This figure also shows that the hardness of the cases peaks at 32-34 HRC, which is the achievable range for this hardening process.

Figure 3b shows the hardness measurements for the second lathe layer at a depth of 0.4 mm. This figure shows that the lowest hardness is 32.9 HRC, corresponding to case 25, and the highest hardness is 38.3 HRC, corresponding to case 21. In general, the hardness of S45C steel cylindrical after arc quenching is higher than 0.2 mm, with the most common range from 35 HRC to 37 HRC, under the same surface-quenching mode. This reflects the trend that the cooling rate of the 0.2 mm layer is lower than that of the 0.4 mm layer. At the 0.4 mm depth layer, the amount of heat absorbed is lower than that of the 0.2 mm layer, and the heat has also spread more widely, so the cooling rate is faster and higher.

Fig. 3c is the hardness measurement result of the third turning layer with a depth of 0.6mm. This figure shows that the lowest hardness is 29.4 HRC corresponding to case number 4 and the highest is 42.6 HRC corresponding to case number 2. In general, the hardness of S45C steel cylindrical after arc quenching when turning to a depth of 0.6 mm is higher than that of the depth cases of 0.2 mm and 0.4 mm with the most frequent range of 35 HRC to 38.5 HRC with the same surface quenching mode. However, the graph also shows a large difference between the experimental cases and the depth cases of 0.2 mm and 0.4 mm, which can be explained by differences in hardness resulting from the heat and phase transformation processes at this layer. When the amount of heat transferred to this depth has decreased so much that there is not enough heat for the complete phase transformation from ferrite and pearlite to the austenite phase, the amount of martensite phase will be less, and the hardness will be lower.

Fig. 3d is the hardness measurement result of the fourth turning layer with a depth of 0.8 mm. This figure shows that the lowest hardness is 21.4 HRC (case 20) and the highest is 43.6 HRC (case 1). The diagram shows a rather large height dispersion due to the obvious difference in surface hardness at this depth layer. This interesting fact further clarifies the hypothesis of heat loss due to heat spreading and the heat-retention effect of the upper layers, such as the 0.2 mm, 0.4 mm, and 0.6 mm layers. That is, when the heat transfer to this depth has decreased so much that there is not enough heat to completely transform the ferrite and pearlite phases to the austenite phase, the amount of martensite phase will be less, and the hardness will be lower.

Fig. 3e shows the hardness measurements for the fifth turning layer at a depth of 1 mm. This figure shows the lowest hardness of 18.9 HRC (case 9) and the highest hardness of 41.9 HRC (case 1). The graph shows the greatest height dispersion, compared to the other graphs, due to the clear difference in surface hardness at this depth. This further clarifies the trend of heat loss with increasing depth, leading to a decrease in surface hardness—especially in cases 9 and 19, with hardnesses of 18.9 HRC and 19.2 HRC, respectively.

In general, **Figs. 3a-3b**, with more even column heights, have the least difference, especially shape b. From **Fig. 3c** with a corresponding depth of 0.6mm, the hardness difference begins to increase, and some cases of hardness decrease appear. In **Figs. 3d-3e**: The hardness difference is larger due to the reduction in heat transfer to these two layers.

Table 3 Experiment parameters designed by using the Taguchi method and average hardness values.

No.	A (ampe)	V1 (mm/min)	V2 (mm/min)	Hardness at 0.2 mm of the depth (HRC)	Hardness at 0.4 mm of the depth (HRC)	Hardness at 0.6 mm of the depth (HRC)	Hardness at 0.8 mm of the depth (HRC)	Hardness at 1 mm of the depth (HRC)
1	110	1	460	32.5	37.8	41.9	43.6	41.9
2	110	2	470	33.6	38.2	42.6	41.8	33.8
3	110	3	480	29.3	35.4	35.9	32.3	22.6
4	110	4	490	31.8	33.5	29.4	26.5	21.7
5	110	5	500	33.9	34.3	32.9	27.9	21.3
6	115	1	470	34.5	37.5	41.7	42.8	37.7
7	115	2	480	29.7	36.8	39.6	41.1	37.5
8	115	3	490	33.5	36.8	38.4	39.5	35.6
9	115	4	500	30.8	36.2	31.6	27.9	18.9
10	115	5	460	31.5	34.7	30.5	30.4	21.6
11	120	1	480	35.2	35.3	39.1	39.6	41.2
12	120	2	490	34.1	34.2	35.8	39.5	37.7
13	120	3	500	32.9	34.5	33.9	35.7	28.5
14	120	4	460	33.3	34.6	35.3	36.7	27.5
15	120	5	470	30.8	34.6	33.8	33.8	28.8
16	125	1	490	37.5	35.9	38.5	31.6	25.6
17	125	2	500	37.7	37.4	36.6	26.9	26.9
18	125	3	460	33.2	36.4	38.1	28.4	22.6
19	125	4	470	33.1	36.8	31.8	24.1	19.2
20	125	5	480	32.5	34.0	33.6	21.4	24.4
21	130	1	500	35.6	38.3	39.5	38.8	32.9
22	130	2	460	36.9	37.0	40.4	35.9	28.6
23	130	3	470	33.8	37.6	37.2	29.6	25.5
24	130	4	480	33.3	34.5	32.9	31.5	21.6
25	130	5	490	35.4	32.9	37.9	30.8	22.9

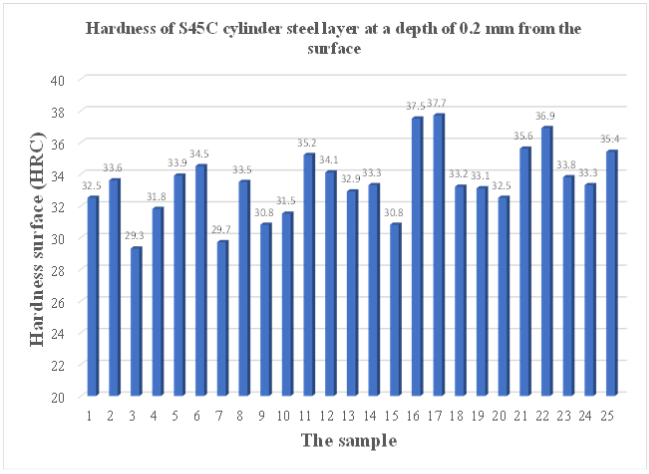

(a)

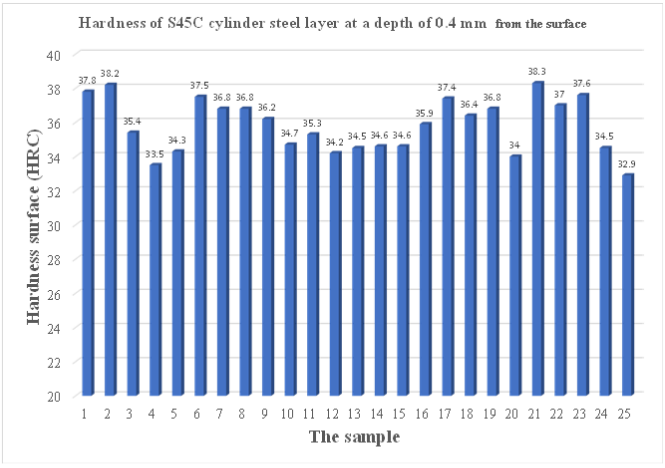

(b)

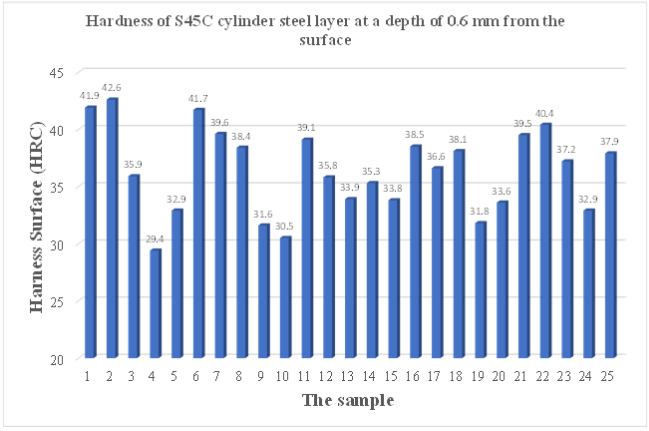

(c)

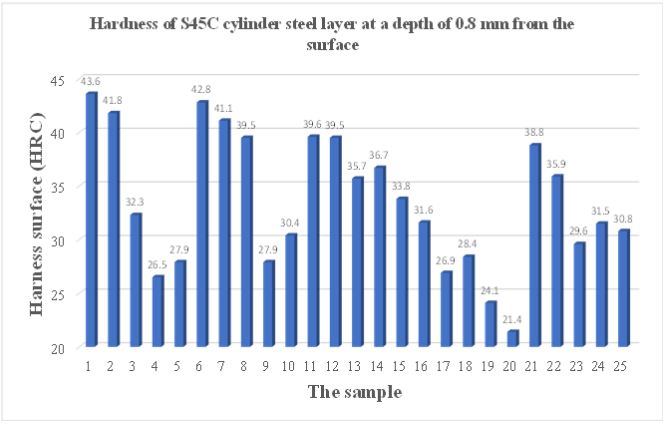

(d)

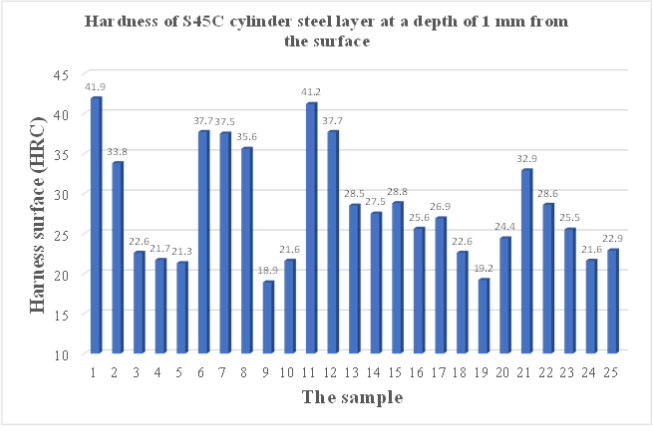

(e)

Fig. 3 Hardness of S45C cylinder steel at the depths from the surface. (a) Hardness at depth of 0.2 mm from the surface, (b) Hardness at depth of 0.4 mm from the surface, (c) Hardness at depth of 0.6 mm from the surface, (d) Hardness at depth of 0.8 mm from the surface, (e) Hardness at depth of 1 mm from the surface

Taguchi method analysis

In addition to hardness evaluation, the impact of surface-quenching process parameters on cylindrical S45C steel was also evaluated. **Figs. 4-8** show the influence of process parameters, including current intensity, axial travel speed, and rotational travel speed of the cylinder. **Fig. 4** shows the impact of the surface-quenching-by-arc process parameters on the 0.2 mm-deep layer. The current intensity has the greatest influence and tends to increase hardness as it increases. This parameter affects the amount of heat generated by the TIG tip, according to the studies of Ninh et al. [15].

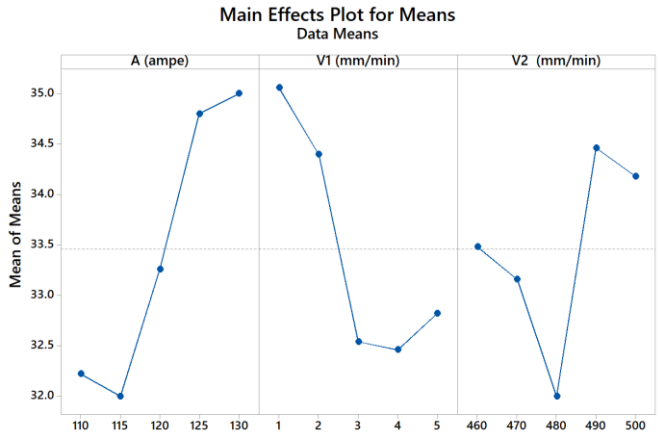

Fig. 4 Main effects plot for Means of the hardness at 0.2 mm of the depth (larger is better).

When the current intensity increases, it generates more heat, thereby increasing the input heat for the surface quenching process by arc on cylindrical S45C steel. For axial travel speed, as V1 increases, surface hardness decreases, especially from 1 mm/min to 3 mm/min, which has the strongest influence. This can be explained by the fact that the width of the thermal field fluctuates from 2 to 6 mm. If the velocity is larger than this range, it may not be effective because two quenched regions appear, and one unquenched region appears on the surface. In V2, this parameter affects the amount of heat input. According to previous studies, when travel speed is higher, heat input is lower, so the surface does not have enough heat to transform to the austenite phase, and the formation of the martensite hard phase is reduced [2, 17]. There are two clear forms of influence of the travel speed on the surface hardness for the depth of 0.2 mm, from 460 mm/min to 480 mm/min the surface hardness tends to decrease due to the decrease in the input heat, from 480 mm/min to 500 mm/min the increase can be explained by the increase can be affected by the amount of heat retained in the surface layer increased without heat transfer deep inside and will consider this hypothesis more closely in the next depth layers. The top of the graph is the optimal value. According to the figure, the optimal value is achieved at a current intensity of 130 A, with V1 = 1 mm/min and V2 = 490 mm/min.

Table 4 shows the Response Table for the Means of the hardness of the 0.2 mm depth layer of S45C steel, with the criterion that the larger the better. This table also shows that the current intensity plays the most important role in the surface layer at this depth; it is still in the strong deformation zone due to the melting zone during quenching. Next is V1, which determines the width of the quenching zone. If the speed is too large, the hardness may not overlap or overlap less. V2 has the least effect on the thickness layer. However, the Delta parameter indicates that the differences among these 3 parameters are not large. All prove that at this 0.2 mm depth layer, the influencing parameters are the same.

Table 4 Response Table for Means of the harness at 0.2 mm of the depth (larger is better).

Level	A (ampe)	V1 (mm/min)	V2 (mm/min)
1	32.22	35.06	33.48
2	32.00	34.40	33.16
3	33.26	32.54	32.00
4	34.80	32.46	34.46
5	35.00	32.82	34.18
Delta	3.00	2.60	2.46
Rank	1	2	3

Fig. 5 evaluated the impact of the arc surface quenching process parameters on the surface hardness of cylindrical steel S45C at a depth of 0.4 mm. For the electric arc intensity, the trend of change is unclear, and the level of influence is unclear when the urban area does not change in a specific direction. This can be explained by the fact that the heat reaching this surface layer fluctuates between overheating, insufficient heat, and just enough heat. Therefore, determining the direction of the influence of the current intensity will not be clear. For axial travel speed, the impact process is more pronounced, with the trend that higher travel speed leads to lower hardness due to the influence of arc width. For the relative travel speed of the TIG head to the cylindrical S45C steel surface, the increasing speed trend will reduce the measured hardness after quenching more clearly than in the 0.2 mm surface layer. The optimal values of the process parameters are 115 A for the current intensity, 1 mm/min for the axial travel speed, and 470 mm/min for V2.

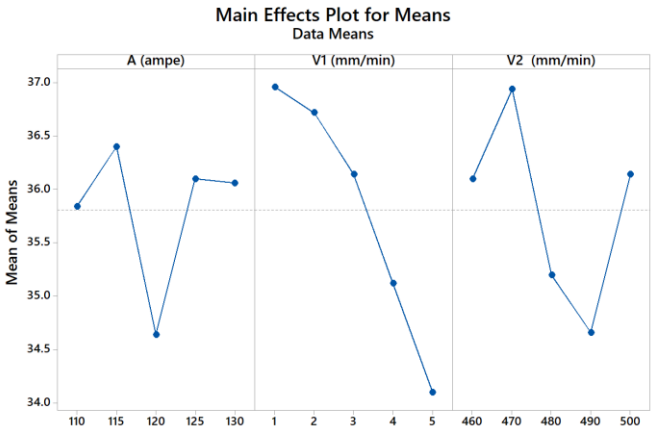

Fig. 5 Main effects plot for Means of the hardness at 0.4 mm of the depth (larger is better).

Table 5 shows the Response Table for Means of the hardness of the 0.4 mm depth layer of hardened S45C steel, with the criterion that the larger the better. This table shows that the axial travel speed plays the most important role for the surface layer at this depth; at this depth, the width of the hardened layer begins to decrease [16, 19]. The rotational travel speed around the main axis has the second-largest influence on layer thickness. Finally, the current intensity. As in the case of the 0.2 mm layer, the magnitude of the differences in the delta values of these three parameters is similar, so their influence is equivalent.

Table 5 Response Table for Means of harness at 0.4 mm of the depth (larger is better).

Level	A (ampe)	V1 (mm/min)	V2 (mm/min)
1	35.84	36.96	36.10
2	36.40	36.72	36.94
3	34.64	36.14	35.20
4	36.10	35.12	34.66
5	36.06	34.10	36.14
Delta	1.76	2.86	2.28
Rank	3	1	2

Fig. 6 evaluates the impact of the arc quenching process parameters on the surface hardness of cylindrical S45C steel at a depth of 0.6 mm. For the electric arc intensity, the hardness decreased when the current increased from 110 A to 120 A, then from 120 A to 125 A, the measured hardness increased slightly, and from 125 A to 130 A, the measured hardness increased sharply. For the axial travel speed, the impact process was similar to that for the depths of 0.2 mm and 0.4 mm. As V1 increased, the measured hardness decreased due to the arc width. For the relative travel speed of the TIG head on the cylindrical S45C steel surface, the graph clearly shows that, as V2 increased, the measured hardness decreased due to a decrease in heat input, consistent with the law of Kurmar et al. [16, 19]. The optimal values of the process parameters were determined as 130 A, 1 mm/min, and 460 mm/min for V1 and V2, respectively.

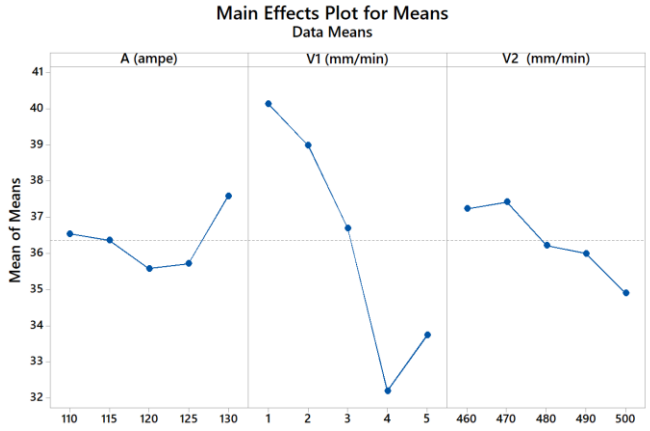

Fig. 6 Main effects plot for Means of the hardness at 0.6 mm of the depth (larger is better).

Table 6 shows the Response Table for the Means of the hardness of the 0.6mm thick S45C steel layer, hardened with the criterion of the larger the better. This table shows that V1 is the most important role for the surface layer at this depth, and the delta value (7.94) is larger than the other two parameters, which are V2 (2.52) and A (2.0). This can be explained by the fact that when the layer is deep, the hardening zone becomes smaller, so the overlapping area between 2 rotations may no longer occur at high V1 speeds, and the ideal velocity is 1 mm/min. V2 remains the second-largest contributor to layer thickness. Finally, the current intensity. Through the tables 4-5, it shows that the delta values of the current intensity and travel speed are low, which can be explained that the depth at levels from 0-0.6 mm are still in the hard zone [16-17, 19, 24].

Table 6 Response Table for Means of harness at 0.6 mm of the depth (larger is better).

Level	A (ampe)	V1 (mm/min)	V2 (mm/min)
1	36.54	40.14	37.24
2	36.36	39.00	37.42
3	35.58	36.70	36.22
4	35.72	32.20	36.00
5	37.58	33.74	34.90
Delta	2.00	7.94	2.52
Rank	3	1	2

Fig. 7 evaluated the impact of the arc quenching process parameters on the surface hardness of cylindrical S45C steel at a depth of 0.8 mm. For the electric current intensity, when increasing from 110 A to 120 A, the hardness tends to increase, possibly because the input heat affecting this layer begins to decrease, so the heat is increased to compensate for the lost heat. From 120 A to 130 A, the hardness decreases because the heat generated is excessive, leading to overheating. For the axial travel speed, the impact process is similar to that for depths of 0.2 mm, 0.4 mm, and 0.6 mm. When increasing the travel speed, the measured hardness decreases due to the influence of the arc width. For V2, the graph also shows the same as the 0.6 mm depth graph, that the hardness decreases with increasing travel speed. The optimum values of the process parameters are 120 A for the current intensity, 1 mm/min for the axial travel speed, and 460 mm/min for V2.

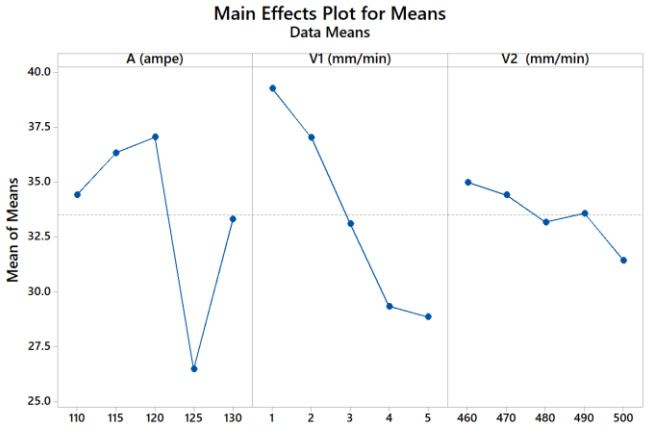

Fig. 7 Main effects plot for Means of the hardness at 0.8 mm of the depth (larger is better).

Table 7 shows the Response Table for Means of S45C steel hardness at 0.8 mm depth, which has been hardened with the criterion of the larger the better. This Table shows that A is the most important parameter with a delta value of 10.58. V1 has the second-largest influence, with a delta value of 10.42. The rotational travel speed is in the third position with a delta value of 3.56.

Table 7 Response Table for Means of harness at 0.8 mm of the depth (larger is better).

Level	A (ampe)	V1 (mm/min)	V2 (mm/min)
1	34.42	39.28	35.00
2	36.34	37.04	34.42
3	37.06	33.10	33.18
4	26.48	29.34	33.58
5	33.32	28.86	31.44
Delta	10.58	10.42	3.56
Rank	1	2	3

Fig. 8 evaluated the impact of the arc quenching process parameters on the surface hardness of cylindrical S45C steel at a depth of 1 mm. For the electric current intensity, the same thing happens as with the depth at 0.8 mm, when increasing from 110 A to 120 A, the hardness tends to increase, possibly because the heat input affecting this layer begins to decrease, so when increasing the heat to compensate for the heat loss, then from 120 A to 130 A, the hardness decreases because the amount of heat generated is quite excessive, causing overheating, so the hardness decreases. For the axial travel speed, the impact similarly at depths of 0.2 mm and 0.4 mm, and 0.6 mm. When increasing the travel speed, the measured hardness decreases due to the arc width. For V2 parameter, the graph also shows that from 460 mm/min to 480mm/min the hardness increases slightly. From 480mm/min to 500 mm/min the hardness decreases due to the decrease in heat input as the travel speed increases. The optimum values of the process parameters are 120 A for the current intensity, 1 mm/min for the axial travel speed, and 480 mm/min for V2.

Fig. 8 Main effects plot for Means of the hardness at 1 mm of the depth (larger is better).

Finally, **Table 8** shows the Response Table for Means of S45C steel hardness at 1mm depth from the surface with the criterion of the larger the better. This table continues to show that the axial travel speed is the most important parameter, and the ideal speed is 1 mm/min. Current intensity has the second-largest influence, and Rotational travel speed is third.

Table 8 Response Table for Means of harness at 1 mm of the depth (larger is better).

Level	A (ampe)	V1 (mm/min)	V2 (mm/min)
1	28.26	35.86	28.44
2	30.26	32.90	29.00
3	32.74	26.96	29.46
4	23.74	21.78	28.70
5	26.30	23.80	25.70
Delta	9.00	14.08	3.76
Rank	2	1	3

In general, through Taguchi method analysis, we can see the influence trends of the parameters of the electric-arc surface-quenching process. For a surface depth of 0.2 mm, the current intensity and the relative motion speed between the TIG head and the cylindrical S45C steel have little effect on the measured hardness because the input heat is too high. The depth from 0.4 mm to 0.6 mm for the cylindrical S45C steel has the clearest trend when increasing the current intensity, causing the input heat to rise, so the obtained hardness decreases. From a depth of 0.8 mm to a depth of 1 mm from the surface, the trend is not clearer; the amount of heat transmitted here can be lost a lot, so it is difficult to identify according to the rule. For the axial travel speed of the TIG head, this is a parameter related to the width of the arc, so it does not affect the input heat much. Throughout the hardness measurement process, the greater the speed, the lower the hardness; the ideal speed is 1 mm/min.

CONCLUSION

This study examined the effects of current intensity, relative travel speed of the TIG tip with the cylindrical S45C steel surface, and axial displacement speed of the TIG tip on the hardness in depth layers of the cylindrical S45C steel surface quenching process. The important findings revealed in this study are:

- With the method of testing the structure of the hardened sample, it was confirmed that there are 3 distinct structural zones, the hardened zone, the heat-affected zone, and the base metal zone. The hardened zone has a structure consisting of martensite, residual austenite, and bainite phases obtained after the arc quenching process from the base metal structure consisting of 2 phases of ferrite and pearlite. The heat-affected zone consists of bainite, pearlite, and ferrite phases. The rapid heating and cooling rates are the main factors causing such phase diversity.
- When evaluating the hardness according to depth with 25 cases, the depth ranges from 0.4 mm to 0.6 mm is more stable and has the highest hardness. The hardness obtained at these 2 depths shows the smallest dispersion, is most stable, and is least influenced by current intensity and travel speed. It is very suitable for surface quenching of cylindrical steel S45C and is also the ideal thickness for surface treatment of details after heat treatment in product processing.
- Taguchi analysis also shows that the axial travel speed follows a certain rule and has almost no effect on the hardness measured according to the depth of the metal layer because it is directly related to the width of the arc.
- Increased current intensity will cause the input heat to increase due to the increased heat generated from the tig head. On the contrary, as the relative speed between the tig head and the cylindrical S45C steel surface increases, the input heat decreases. Both current intensity and travel speed factors strongly affect the hardness obtained and have a difficult-to-determine rule between different depth layers, except for the 0.4 mm and 0.6 mm layers.

These findings provide valuable insights for industries seeking cost-effective alternatives to laser or electron-beam hardening, especially for applications requiring high hardness at lower processing costs.

Acknowledgements: The authors acknowledge the funding from HCMC University of Technology and Education under grant number T2024-32 for this study

REFERENCES

1. M. Hruška, M. Vostřák, J. Tesar: IOP Conference Series: Materials Science and Engineering. 461, 2018, 012027. https://doi.org/10.1088/1757-899X/461/1/012027
M.J. Schneider, M.S. Chatterjee: Introduction to surface hardening of steels. In *Steel Heat Treating Fundamentals and Processes,* ASM International: Ohio, 2013, p. 389-398. https://doi.org/10.31399/asm.hb.v04a.a0005771
2. D. Ren, P. Zhang, J. Yu, Y. Yao, X. Li: X: Frontiers in Physics, 10, 2022, 1115447. https://doi.org/10.3389/fphy.2022.1115447
H. Li, H. Zhou, D. Zhang, et al.: Journal of Materials Engineering and Performance, 30, 2021, 2238–2244. https://doi.org/10.1007/s11665-021-05505-w
3. M.K. Lee, G.H. Kim, K.H. Kim, W.W. Kim. Surface and Coatings Technology, 184(2–3), 2004, 239-246. https://doi.org/10.1016/j.surfcoat.2003.10.063
4. S.Q. Lu, L.H. Chiu, H.H. Cheng: Materials, 18(5), 2025, 1045. https://doi.org/10.3390/ma18051045
5. S. Valkov, M. Ormanova, P. Petrov: Metals, 10(9), 2020, 1219. https://doi.org/10.3390/met10091219
6. K. Peng, D. Yu, P. Zhang, L. Wang, Z. Liao, Z. Lu, G. Wu, Ch. Song, L. Li: Surface and Coatings Technology, 473, 2023, 130029. https://doi.org/10.1016/j.surfcoat.2023.130029
7. E.N. Safonov: Metal Science and Heat Treatment, 47, 2005, 434–439. https://doi.org/10.1007/s11041-006-0007-0
8. E.N. Safonov, Y. Gordon: AIP Conference Proceedings, 2456(1), 2022, 020042. https://doi.org/10.1063/5.0074746
9. E.N. Safonov, M.V. Mironova: AIP Conference Proceedings, 2456(1), 2022, 020032. https://doi.org/10.1063/5.0074741
10. A.N.M.D. Idriss, S. Kasolang, M.A. Maleque, R.M. Nassir: Jurnal Tribologi, 29, 2021, 96-116.
11. E.N. Safonov, M.V. Mironova: Materials Science Forum, 989, 2020, 318-323. https://doi.org/10.4028/www.scientific.net/MSF.989.318
12. V.K. Goyal, P. Ghosh, J.S. Saini: Journal of Materials Processing Technology, 209, 2009, 1318–1336. https://doi.org/10.1016/j.jmatprotec.2008.03.035
13. N.T. Nguyen, A. Ohta, K. Matsuoka, N. Suzuki, Y. Maeda: Welding journal, 78, 1999, 265s-274s.
14. K. Sudhir, P.K. Ghosh, R. Kumar: Journal of Materials Processing Technology, 249, 2017, 394-406. https://doi.org/10.1016/j.jmatprotec.2017.06.035
15. A.E. Mikheev, et al.: Welding International, 17, 2003, 570-572. https://doi.org/10.1533/wint.2003.3162
16. K. Sudhir, P.K. Ghosh. International Journal of Fatigue, 116, 2018, 306-316. https://doi.org/10.1016/j.ijfatigue.2018.06.036
17. R. Kumar, P.K. Ghosh, S. Kumar: Journal of Materials Processing Technology, 240, 2017, 420–431. https://doi.org/10.1016/j.jmatprotec.2016.10.020
H. Khanna, H. Singh: International Scientific Journal of Engineering and Management, 04, 2025, 1-6. https://doi.org/10.55041/ISJEM02349
18. J. Joshi, S.K. Sahu: Experimental Heat Transfer, 35(7), 2021, 938–963. https://doi.org/10.1080/08916152.2021.1995082
19. D.J. Kim, S. Jeong, T. Park, D. Kim. International Journal of Heat and Fluid Flow, 79, 2019, 108458. https://doi.org/10.1016/j.ijheatfluidflow.2019.108458
20. B. Meyghani, M. Awang: Archives of Computational Methods in Engineering, 27, 2020, 563-576. https://doi.org/10.1007/s11831-019-09319-x
21. V.-T. Nguyen, P.S. Minh, H.-S. Dang, N. Ho: PLoS ONE 19(12), 2024, e0314648. https://doi.org/10.1371/journal.pone.0314648
22. L. Orazi, E. Liverani, A. Ascari, A. Fortunato, L. Tomesani: CIRP Annals, 63(1), 2014, 233-236. https://doi.org/10.1016/j.cirp.2014.03.052
23. I. Basori, W.D. Pratiwi, S.T. Dwiyati: Journal of Physics: Conference Series, 1402(5), 2019, 055102. https://doi.org/10.1088/1742-6596/1402/5/055102